10

Looking at Remote Sensing the Timing of an Organisation's Point of View and the Anticipation of Today's Problems

Y. A. Polkanov
Private
Belarus

1. Introduction

Any remote measurement involves recording a signal from some sort of continuous medium of atmosphere in general. This is a signal which possesses a certain temporary structure, and in turn, this temporary structure bears some information on the spatial inhomogeneities of the continuous medium's structure and the arrangement of its specific properties (e.g. optical, microphysical, etc.). The nature of these structures depends upon the thermodynamic processes in the environment and the sustainability of these processes. Thermodynamics is the inevitable factor for their participation and it demands an account of the processes having obviously extended character. The classical approach assumes some property of the environment at a certain point in time and at a certain point in the medium. In accordance with this, today's remote measurements use the digitisation of a received signal with certain stable time step of digitisation. All efforts have been consolidated so as to receive the medium-sized digital signal samples which have been reduced to an acceptable size. Such an approach has at its core a logical contradiction – information of the properties of an extended environment trying to get at the point where it actually is not. There is something that is subject to consideration absolutely from other positions and the use of other tools. Measurements should be conducted in a certain 'visible' volume which provides the effect of the 'presence' of the medium and which has a specific thermodynamic 'meaning'; that is, that it has some of the 'thermodynamic memory'. These volumes should be comparable (in length) to the length of all zones' (lines') measurements. However, this generates a new contradiction which arises when the discretisation signal is read out. How should one get a spatial resolution close to the size of the inhomogeneity with the signal time's discretization using intervals commensurate with the length of the track measurements? This contradiction can be resolved only indirectly, using a principle that can be called a kind of 'principle of relativity'. Here, we use a pair of discrete samples which have a common border and a second boundary which is different to the desired step of discretization. This approach provides for the possibility of studying the environment and its irregularities while maintaining the required signal/noise ratio.

The internal logic of this approach abstracts the properties of the medium at the point and then moves on to the study of the environment as a self-organising system. The 'test body' of such research is the structure of the inhomogeneities of the medium. The nature of this

structure is directly dependent upon the thermodynamic stability of the environment. Changes within the structure of the inhomogeneities are more mobile and are preceded by changes in the thermodynamic state of the environment as a whole. We take this as an axiom. As such, the structure of the inhomogeneities is central to the prediction of processes within the environment. This becomes especially important during the development process of a catastrophic scenario. Their nonlinear nature makes standard methods for the analysis of irregularities ineffective because of the number of initial assumptions, which often only apply to the environment in the classical sense. Therefore, I propose a structural-statistical method for analysing the structure of inhomogeneities.

2. Methodological approach

2.1 Measurements

The results of the actual measurements of laser systems for the remote-sensing of the atmosphere are used to verify the proposed approach. Currently, the laser systems for remote-sensing use high-power pulsed lasers, and the backscattering signal is written with a certain sampling step corresponding to the required spatial resolution. Moreover, the growth of the length of the track-sensing leads to a disproportionate growth of the power source and the dynamic range of the incoming signal. It also causes the multiple scattering effects which can be difficult to take into account.

The new approach is based upon the use of a low-power radiation source (for example, a source of white light) within the specified parameters of the gating. The dark pulse of the continuous light source has a duration equal to usual laser pulse lidar (about 10^{-8} c). The time interval between the dark pulses is close to the time of the radiation propagation in an area where we can neglect the multiple scattering. The digitisation of the remote-sensing signal can be performed with standard digital systems (a constant gate) as well as with systems based on the proposed approach (an increasing gate).

I propose to restore the average characteristics of the medium to long sections of a length close to the length of the track measurements. This will significantly increase the accuracy of the reconstruction of the properties of the real heterogeneous medium. Signal processing assumes the creation of the registration system with an increasing time-step gate of the incoming signal (the one-dimensional case).

The comparative calculation of the required radiation power was held for a given signal/noise ratio for different average atmosphere extinction coefficients $\sigma = 10^{-2},..., 1\ km^{-1}$ (the old and new systems).

For high transparency ($\sigma = 10^{-2}\ km^{-1}$), the maximum length of the zone of measurement is chosen equal to the length of the layer of a dense atmosphere, significantly affecting the scattering signal (L_{max} = 30 km). To muddy the atmosphere, this distance is set by the condition that the optical depth does not exceed $\tau = 2\sigma L = 10$. This allows us to consider the scattering of the signal with an accuracy of 0.05% and to neglect the signal over large distances. Single scattering occurs with the condition $\tau = 2\sigma L < 3$ (Kovalev, V. A., 1973; Ablavskij, L. M. and Kruglov, P. A., 1974). The calculations were made on the assumption of single scattering. The data obtained is used only so as to illustrate the detected trends ($\tau > 3$).

All estimates are carried out based on an expression derived from the lidar equation for systems I and II (Polkanov, Y. A. and Ashkinadze, D. A., 1988):

$$n_i = AW_1 (e^{-2\sigma li} (1 - e^{-2\sigma lc}))/L^2 \quad (1)$$

$$n_{i1,i2} = AW_2 \sum_{i=l_T/l_s}^{L_{1,2}/l_s} \left(e^{-2\sigma li} \left(1 - e^{-2\sigma lc} \right) \right) / \left(l_i + l_s / 2 \right)^2 \quad (2)$$

Where n_i, n_{i1},i_2 - obtained discrete values from the scattering signal (number of photon counts); A – a coefficient which brings together the supporting equipment characteristics; $W_{1,2}$ – the power of the laser radiation; L – the distance from the centre section of the route, by which the signal is recorded; l_i - the distance from the system to this site; l_s – the length of the section; l_T - the length of the shadow zone of the lidar where the signal is not recorded (600 m). We assume for the system that II $L_2 > L_1$, $(n_{i2} - n_{i1}) = n_i$. An advanced assessment of the relative measurement error of the signal (δ_i, δ_{ix} for System I and System II) was conducted on the basis the expressions (Polkanov, Y. A. et al., 1985; Polkanov, Y. A. et al., 2004):

$$\delta_i = t_\beta((n_i - n_n)^{1/2})/ n_i \quad (3)$$

$$\delta_{ix} = t_\beta((n_{ix} - 2B_x n_n)^{1/2})/ n_{ix} \quad (4)$$

Where t_β – the coefficient equal to the probability of the matching error computed to its actual value (if $t_\beta = 2$, the probability is equal to 0.95). The necessity of this evaluation is due to the appearance depending δ_{ix} (t) for system II (signal/noise = const). This is due to the progressive rise in the value of the time intervals recording the scattering signal (with the digitisation step – t_s). The level of background illumination takes into account the introduction of the coefficient B = f (t) in (4). The measurement error for individuals counts the signal and background-level measurement errors, becoming comparable for large intervals of T_S. They are significantly higher than the level of internal noise (in. ns.) receiving system (in this case, $n_{in.ns} \sim 0.1$, t_s = 0,4 ms). Moreover, the summed value of the signal increases to a certain point in time, reaching a maximum level of accumulated signal (Kovalev, V. A., 1973; Ablavskij, L. M. and Kruglov, P. A., 1974). However, the level of background illumination increases linearly with time. The calculations used the results of the actual measurement system I (n_i, n_b, σ). The coefficient A in (1) is also evaluated and used in subsequent calculations for the system II (2).

2.2 Processing

The following processing scheme was assumed: the initial signal (as a time function) → the generalised structure of a signal → an elementary cell of the signal structure. The multiplication of such cells allows the complete restoration of the characteristic structures in the supervised space.

The indicator of the time stability of the signal structure was the dispersion of the components of the elementary cell of a signal structure. If the dispersion exceeds an interval between elements of the revealed cell then the structure is unstable. The correlation of the generalised frequency structure of a horizontal signal and the generalised parameter which fixes the thermodynamic stability of the environment is a characteristic sign of the self-organising of the environment.

The basis for the reception of new results is a series of works on the laser sounding of the atmosphere in stable nightime conditions. This has allowed the development of certain methods for the structural-statistical processing of an initial remote signal. The aim is to reveal the signs of the steady organisation of the frequency structure of environmental inhomogeneities.

The generalised regular structure comes from the summary of the sequence of the discrete readouts. They were received by the scanning of the investigated volume of the environment in a horizontal plane to a set of directions and with the set angular permission (Polkanov, Y. A. et al., 1989).

During the following stage, the signal is represented in the form of a regular structure of local maxima and minima. There was a separate analysis of the 'plus' and 'minus' structures (Polkanov, Y. A. and Kudinov. V. N., 1989).

These components behave as whole object and are registered as a uniform regular structure (type harmonious) only in the case of a steadily vertical stratified environment. When the infringement of the stability of the stratification of environmental communication between the 'plus' and 'minus' structures decreases, they become increasingly independent of one another other. The degree of such dependence can be characterised by a certain numerical parameter (Polkanov, Y. A. et al., 1991; Polkanov, Y. A. et al., 2009).

The thermodynamic stability of the environment and its stratification can be characterised numerically by a special generalised parameter on the basis of Richardson's number. With the infringement of the thermodynamic stability of the environment, this parameter adopts wavy characteristics on a vertical plane. The length of such a 'wave' with the falling of the environmental stability was decreased.

The integrated regular structure of vertical thermodynamic distribution is an indicator of such stratification of the environment.

It is possible to speak about the communication of the optical structure horizontal stability with the vertical stability of the thermodynamic structure of the environment and its stratification as being an indicator of such stability (Polkanov, Y. A. et al. 1989).

Besides this, the infringement of the stability of the environment leads to the infringement of the stability of the revealed structure and the occurrence of obvious anomalies within the structure (Polkanov, Y. A. et al., 1991; Polkanov, Y. A. et al., 2008) whose behaviour can provide information on the direction of the reorganisation (self-organisation) of the environment.

3. Update of the concept of signal/noise ratio

It transpired that the signal/background noise ratio (S/N) is ambiguous due to the accuracy of the measurement of the scattering signal by the use of the extended strobe. Indeed, when t_i = const and S/N = const for the system I, this automatically means the constancy accuracy of the scattering signal (∂ = const) from strobe to strobe. For example, we set ∂ = 10% for $\sigma \sim 0.1$ km^{-1} for the basic equipment (system I) with S/N = 10. For the systems of type II, the signal is accumulated over time intervals the value of which is not constant, but rather varies in such a way that satisfies the condition: t_i (n) = (t_i (n-1) + t_i)) is t_i (n)> t_i (n-1). The

essential point here is the rise of the level of the recorded background illumination with the increasing duration of the strobe. The scattering signal increases from the strobe to strobe – in general – to the so-called maximum accumulated signal (Kovalev, V. A., 1973).

The background illumination level is significantly higher than the corresponding internal noise receiver (in.ns = 0.1 for t_i = 0.4 ms). It exceeds the signal of system I, with a point, but is comparable with the level of the scattering of the signal of system II ($\tau < 3$). In this case, the accuracy of the scattering signal and the background are similar, and they can be used as useful signals on an equal basis.

In fact, we have a mixture of two signals - the scattering signal and the background signal. Their value increases from strobe to strobe and the first of them (S) rises to a certain level (W_{max}) whilst the second of them (b) increases linearly with time and indefinitely.

In these circumstances, the accuracy of the scattering signal increases when S/N = const (1 because a strobe the length of the time of registration is increasing.

Thus, there is a new dependence - ∂ (t) which was previously unavailable for system I . Table 1 lists the measurement error depending upon the distance l_s (n) corresponding to the interval gating t_s (n), if S/N = 10 = const, for $\sigma = 0.1$ km^{-1}, $n_b = 50$, $t_i = 0.4$ s.

L (km)	**1**	**2**	**3**	**4**	**5**	**10**
δ,%	3,7	1,7	1,3	1,2	1,1	0,8

Table 1. The measurement error decreases with increasing interval gating.

Model calculations showed that the measurement accuracy of the scattering signal for system II is several times higher than the measurement accuracy for system I. This means that for the same radiation power of remote systems, greater measurement accuracy is achieved for systems of type II through special time organisation and its recording of the digitised signal ($\partial_{II} \neq \text{const} \leq \partial_I = \text{const}$).

We can talk about the actual incompleteness of the concept of the signal/background ratio for the registration systems of type II when the strobe length (a single reference signal) depends upon the position of the laser pulse on a remote line sensing. Moreover, it is possible that the signal/background ratio is less than unity but that the measurement accuracy remains high. This is possible when the signal/internal noise ratio (S/in.ns) and the background/internal noise ratio (b/in.ns) is much higher than 1. An example of such situations is provided by Table 2.

L(km)	**1**	**2**	**3**	**4**	**5**	**10**
S/N	1,23	0,81	0,65	0,55	0,49	0,33

Table 2. Signal/background ratio, depending upon the length of the strobe (km) and where the measurement error δ = 10% (const).

The obtained simulation results suggest that the measurement accuracy was higher than expected, if only to carry out the calculation of the signal/background ratio for systems of type II.

4. Data analysis and simulation results

Model calculations based on the data obtained by the laser probing of the atmosphere by means of system I with an output power equal to 0.67 mW (Ashkinadze, D. A., Belobrovik, V. P., Spiridovich, A. L., Kugeiko, M. M. and Polknov, Y. A., 1980; Ashkinadze, D. A and Polkanov, Y. A., 1980; Polkanov, Y. A. et al., 1985; Polkanov, Y. A and Ashkinadze D. A., 1988; Polkanov, Y. A. et al., 1991).

The results of real lidar measurements are used to model the time organization of the proposed emission and detection. Lidar has the following characteristics:

- Radiation source:

Radiation energy E = 0.01 J;

Pulse duration T_o = 15 ns;

Pulse repetition frequency f = 50 Hz.

- Receiving system:

Diameter of the receiving mirror D = 0.1 m;

Operation of a photomultiplier tube (PMT) - an account of the photons;

Quantum efficiency of PMT η = 0,1;

- Recording equipment:

Time interval signal detection in single channel t_i = 0,4 mkc;

Number of cycles of signal m – 3000;

Total measurement time t = 60 s (Polkanov, Y. A. et al., 1985).

The measurement conditions corresponded to the registration of a Poisson flow of the signal photons (Polkanov, Y. A., 1983). The number of the cycles of the accumulation provided a measurement error of no worse than 50%.

Fig. 1. The lidar scheme, with a separated transmitter and receiver.

The simulation results are presented as a set of tables.

4.1 The simulation results of the proposed temporal organisation of the detected signal

We shall call this remote sensing system (lidar) as a base 'System I' (the old system), and a system with increasing intervals of registration (strob) 'System II' (the new system).

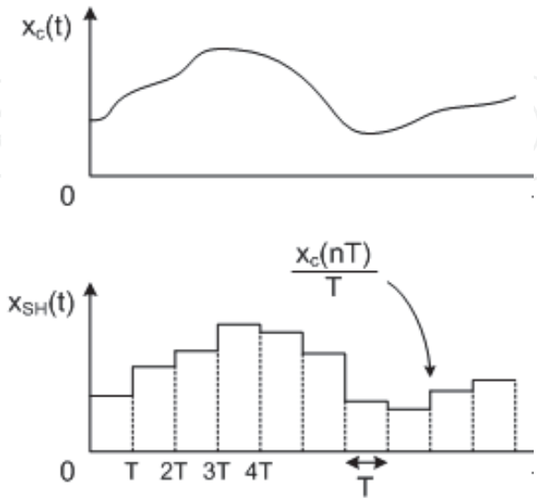

Fig. 2. Discrete-time signal $x_c(t)$ processing for System I.

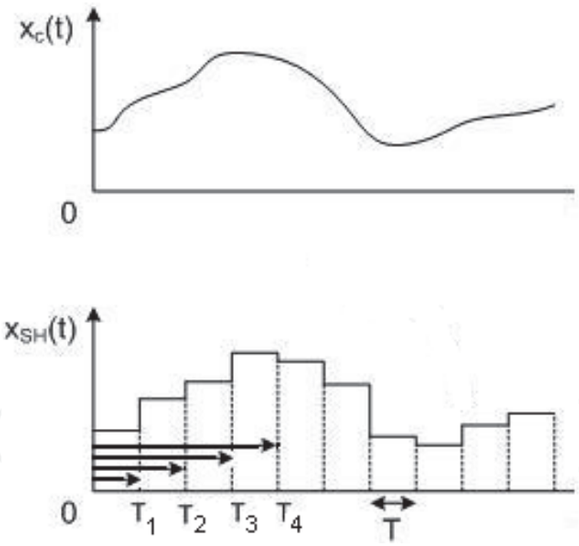

Fig. 3. Discrete-time signal $x_c(t)$ processing for System II (T_1 = T, T_2 = 2T, T_3 = 3T, T_4 = 4T).

The calculation of the signal/background ratio and the corresponding measurement errors of the scattering signal is carried to the appropriate conditions of 'twilight' (∂_1) and 'cloudy day' (∂_2) when the level of background illumination increases by two orders of magnitude. The following table shows the dynamic range (DR) and signal/background ratio for the a wide range length of the path sounding (L) for each value of the extinction coefficient (σ) from the real range. The level of illumination is selected for the corresponding conditions with a high transparency of the atmosphere (~ 10^{-2} km^{-1}).

Fig. 4. Organisation model of the discrete-time signal processing.

σ (km^{-1})	L(km)	1	2	3	4	5	10	15	30	DR
	s/n	19,00	9,40	6,50	5,00	4,00	3,00	1,30	0,60	29
0.01	∂_1 (%)	2,60	2,10	2,01	2,03	2,06	2,36	2,62	3,29	29
	∂_2 (%)	8,34	8,87	9,94	11,10	12,15	17,21	20,69	28,75	29
	s/n	164,30	82,30	54,80	40,00	31,80	15,10	9,90	4,80	34
0.1	∂_1 (%)	0,84	0,66	0,63	0,63	0,63	0,63	0,65	0,66	34
	∂_2 (%)	1,24	1,25	1,36	1,51	1,65	2,29	2,79	2,97	34
	s/n	363,60	166,70	106,00	75,50	59,40	27,70	18,10	15,90	23
0.3	∂_1 (%)	0,56	0,46	0,44	0,44	0,44	0,44	0,45	0,46	23
	∂_2 (%)	0,70	0,66	0,63	0,87	0,95	1,26	1,52	1,61	23
	s/n	419,80	156,80	94,80	66,70	52,10				8
1.0	∂_1 (%)	0,52	0,46	0,46	0,47	0,47				8
	∂_2 (%)	0,63	0,77	0,87	0,98	1,06				8
σ(km^{-1})	L(km)	0.1	0.2	0.3	0.4	0.5				8
	s/n	420000	156000	95000	66000	52000				8
10.0	∂_1 (%)	0,05	0,05	0,05	0,05	0,05				8
	∂_2 (%)	0,05	0,05	0,05	0,05	0,05				8

Table 3. The measurement error (∂) of the signal/noise ratio (S/N) and the dynamic range (DR), depending upon the length of the path sounding (L) and the extinction coefficient of the medium (σ).

The measurement error of these conditions is calculated by formula (1) and does not exceed a few percent. For most cases, we can assume that it will be less then common instrument

errors of the detecting apparatus. The error increases with the daytime measurements (at the same transparency), but by no more than an order of magnitude; its increase is insignificant for the extinction coefficient range σ = 1-10 km^{-1}. The dynamic range of the signal/background ratio is small and varies with changing conditions in the atmosphere; it is much smaller than in the case of system I (DR = 8 - 34).

The data obtained suggests the following conclusions:

1. The use of 'growing' of the proposed type of strobe allows for the measurement of the single-scattering signal with a high precision. Measurements become possible in the daytime.
2. Small dynamic range of the signal/background ratio will simplify the recording equipment without compromising the accuracy of the measurement by eliminating any redundant requirements for its performance.
3. The use of this approach shifts the problem of increasing the measurement accuracy from the area associated with the environment to the area associated only with the instrumental capabilities of the remote systems (i.e. they are more controlled).
4. An additional advantage of the developed approach is the small dynamic range of change of the error signal scattering, depending upon the distance to the considered section of the remote sensor.

The accuracy varies slightly from a strobe to strobe on most of the track soundings. This provides significant advantages for the correctness of the subsequent interpretation of the data.

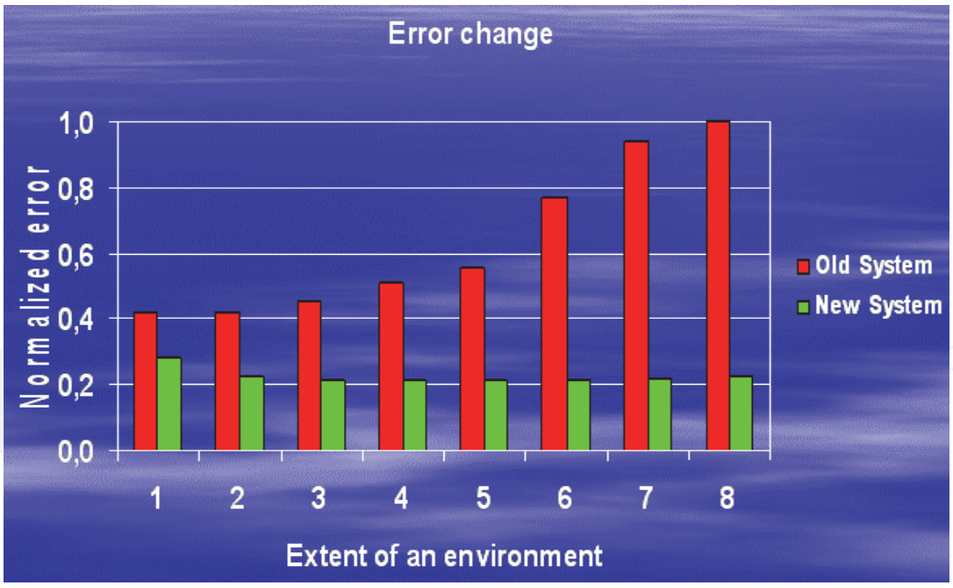

Fig. 5. Normalised error of measurement, depending upon the length of the path sounding.

The analysis of the dynamic range of the scattering signal also shows the advantages of system II. The dynamic range of the signal does not exceed the value 10^2, compared with value 10^6 for systems of type I. Table 5 shows the value (DR) of the scattering signal and the background level for system II. In our case, the range for backlight can reach 10^3, remaining several orders of magnitude lower than for the scattering signal of system I.

σ(km^{-1})	L(km)	1	30	DR
0.01	signal	6462	15600	72
0.01	background (noise)	850	25000	900
σ (km^{-1})	**L(km)**	**1**	**2**	**DR**
0.1	signal	57580	113730	59
0.1	background (noise)	850	25000	900
σ(km^{-11})	**L(km)**	**1**	**17**	**DR**
0.3	signal	127465	217625	29
0.3	background (noise)	850	14150	283
σ (km^{-1})	**L(km)**	**1**	**2**	**DR**
1	signal	147150	190310	6,5
1	background (noise)	850	4150	24,4
σ (km^{-1})	**L(km)**	**0,1**	**0,5**	**DR**
10	signal	14739000	19004096	6,4
10	background (noise)	85	415	24,4

Table 4. The number of the signal count (n_s) and the background (n_b) for the photon counting mode, and the dynamic range (DR), depending upon the extinction coefficient of the medium (σ).

σ(km^{-1})	L(km)	1	2	3	4	5	10	15	30
	Δl_s(m)	10	43	97	18	29	125	320	169
0.01	Δt_s(ns)	67	287	647	120	193	233	2130	1130
	ΔP_{nbg}	8	36	81	15	24	104	26	141
	Δl_s(m)	2	6	16	36	70	40	500	9700
0.1	Δt_s(ns)	13	40	107	240	467	266	3300	64700
	ΔP_{bg}	2	5	13	30	58	733	417	8083
	Δl_s(m)	0,6	4,4	18,0	60,0	190,0			
0.3	Δt_s(ns)	4	29	120	400	1270			
	ΔP_{nng}	065	367	15,0	50,0	158,0			
	Δl_s(m)	0,7	21,7	730,0	50,0		**N ex.n. = 0,3**		
1.0	Δt_s(ns)	4,7	145,0	4870,0	333,0		**$\Delta P_s > \Delta P$ex.n.**		
	ΔP_{nbg}	066	18,0	608,0	42				
σ(km^{-1})	**L(km)**	**0.1**	**0.2**	**0.3**	**0.4**		**ΔP_s = 100, 10, 1**		
	Δl_s(m)	-	0,3	3,9	6,0				
10.0	Δt_s(ns)	-	2	26	40,0				
	ΔP_{nbg}	-	0,2	2,6	5,0				

Table 5. The required increase of the signal sampling interval (space, time) which provided the desired signal increase and its corresponding background increase.

To estimate the limiting possibilities of system II, we calculated the allowable spatial resolution of the remote sensing under various conditions in the atmosphere. The calculation was performed as follows:

1. A constant increment of the scattering signal ΔP_s is posed.
2. The increment area sounding (ΔL) which provided a signal increment (ΔP_s) for certain values of the extinction coefficient (σ) and the length of track is then identified.
3. The increment ΔL thereby obtained is taken as the minimum spatial discretisation step track at a distance L.
4. The necessary step time sampling rate is determined for the recording equipment (Δt_s) on the basis of the obtained values, ΔL.
5. The increment background illumination (the number of the background count ΔP_b) is determined on the basis of the intervals' increment, Δt_s

To estimate the limiting possibilities of system II, we calculated the valid value of the spatial resolutions under various conditions in the atmosphere. The calculation was performed as follows: the value of ΔP_s given as the number of samples (100, 10, 1), with the transition from one value to another. The value ΔP_s does not exceed step ΔL spatial discretisation achieved the basic apparatus in version of the system I. The calculation results for $W_0 = 0.67$ mW are shown by Table 6. The increments ΔP_s certainly took higher increments due to the internal noise receiver. This was the case for $\sigma = 10^{-2}$ km^{-1} to L = 30 km, for $\sigma = 0.1$ km^{-1} to L = 15km, for $\sigma = 0.3$ km^{-1} to L = 5 km, and for $\sigma = 1$ km^{-1} to L = 4 km.

We have exceeded ΔP_s over ΔP_b in all cases (to dusk) when $\Delta Pc = 100, 10$. This is much less than was the case for system I. The simulation results suggest that there is a real opportunity to provide the increment of the scattering signal on the increment of the recorded background illumination ($\Delta P_s > \Delta P_b$) for a wide range of conditions by the adjustment of the values Δt. At the same time, the allowed (minimum) time increments Δt_s (increments for the individual remote-sensing signal samples) do not exceed – in this case – hundreds of nanoseconds (in the zone of single scattering).

4.2 The simulation results of the proposed organisation of the sounding signal radiation

The proposed approach can be applied not only to the organisation of the temporary registration of the incoming signal (in the case of passive systems), but also to the temporary organisation of the radiation of the sounding signal (in the case of active systems).

We consider three types of organisation of the radiation source:

- Pulsed light source (laser) with a pulse substantially shorter than the sounding track (type I).
- Pulsed light source (laser) with a pulse substantially equal the sounding track (type II).
- Long pulsed light source with a repetition-rate that ensures the duration of the interval between the pulses is equal or near to the pulse length of type I (type III), dark pulse laser (Mingming, Feng, Kevin L. Silverman, Richard P. Mirin and Steven T. Cundiff, 2010).

Again, asAs before, the basic system is taken to be a real system of type I (V. E. Zuev, M. V. Kabanov, 1977) with a constant duration of strobe (t_s = 0.4 ms) and the characteristics

	1	2	3
Duration of the radiation impulse	15 ns	18 μs	18 μs
Length of the radiation impulse	4.5 m	5.4 km	5.4 km
Radiation Energy	0,01 J	18 μsJ	18 μJ
Radiation impulse power	667 kW	1 W	1 W
Registration strobe duration	0.4 μs	0.4 μs	0.4 μs
Registration strobe length	60 m	60 m	60 m
Strobe numbers on a line	90	90	90
Line length	5.4 km	5.4 km	5.4 km
Measurement total time	60 s	60 s	60 s
Number of the accumulation cycles	3000	514000	3300000
Frequency of the impulses	50 Hz	8.57 kHz	55.5 kHz
Spatial interval between impulses	» 5 km	30 km	« 5 km
Total radiation energy	30 J	9.25 J	60 J
Average radiation power	0.5 W	0.15 W	1.0 W
Background readout number in a strobe	50	8570	55500
Signal readout number in a strobe (min)	83	4258	182600
Measurement error	33%	7%	0.6%
Background readout number/parcel	0.017	0.017	0.017
Number of signal readout number/parcel (min)	0.028	0.008	0.055

Table 6. The calculated characteristics of the equivalent remote-sensing systems of type I, II and III.

described above. In addition, we used data obtained by probing the system in advanced atmospherics with the extinction coefficient $\sigma = 0.1$ km^{-1}.

The comparative evaluation of the above types of systems was carried out under the assumption used that in the future there would be a a source of continuous light source radiation with a radiated power ~ 1W, since this energy is easily attainable at the present level of the laser system development. We select a maximum . The length of the route maximises the accumulated signal for the conditions of a single scattering ($\tau = 2\sigma l \leq 3$). For system III, an assumption is introduced – the interval between pulses (60 m) does not affect the accumulated signal for distances greater than the path length of the maximum accumulation ($L_{max} \sim \tau = 3$) (Polkanov, Y. A. et al., 2007; Polkanov, Y. A. et al., 2008).

The temporal organisation of the remote-sensing signal reception, the level of background illumination, and the total measurement time is expected the same for all the simulated systems. This data is shown by Table 7, which summarises all of the necessary characteristics for comparison.

The analysis of this data allows us can conclude that to provide the necessary signal levels due to the growth of the pulse repetition rate, the frequency of system II should be raised to 8.57 kHz, and that of for system III to 55.5 kHz. These limitations are needed so as to exclude the presence on the track sensing of the two light pulses (for systems I and II) or the dark pulses (for system III).

The computed frequencies provided a growing number of background counts (compared with system I) for system II (171 times) and system III (- 1100 times). Accordingly, the number of signal photon counts was increased in 51 and 2200 times. This allows us to reduce the measurement error from 33% to 7% and 0.6% respectively for systems II and III. The evaluation shows that the use of systemsusing a system of type II andor type III – even with a radiation source with a capacity of 1 Watt – can significantly improve the measurement accuracy of the scattering signal, relative to the system I (radiation power ~ 1 Watt).

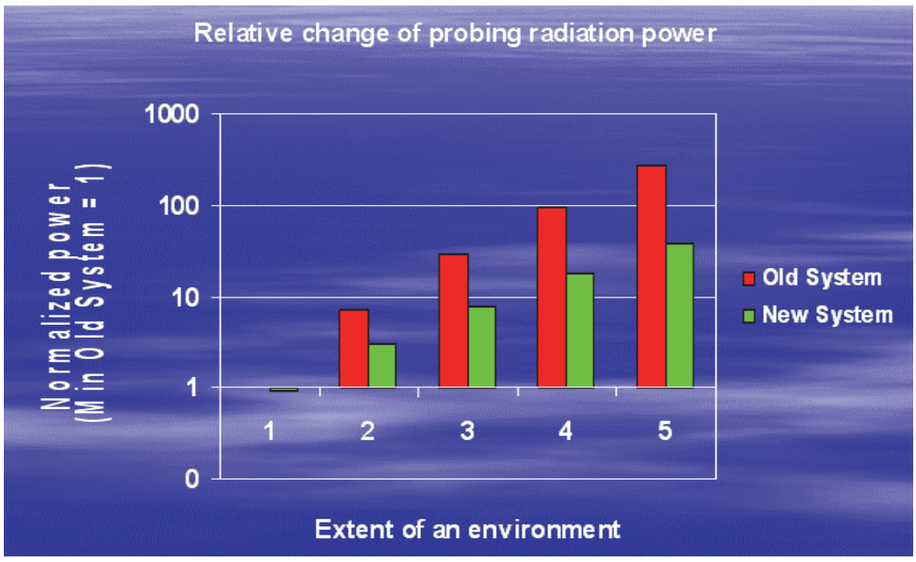

Fig. 6. Normalised power systems I (old) and II (new) as a function of environmental conditions (σ=0,01-1 km^{-1}) at the same signal/noise ratio.

This is achieved through the formation of the continuous emission of long pulses (dark pulses) with a high repetition rate. It allows for a fixed measurement time (60 s) registering a much larger number of photons. Thus, we can reduce the required power of the radiation source. It is interesting estimating the maximum possible repetition rate laser pulses for system II. The pulse length varies from one pulse to the next the length of the registration strobe (single reference signal) changes from one strobe to another gate. To eliminate the effect of the scattering signal from the previous pulse, the interval between pulses (l_Δ) was chosen according to the condition: σ (l_Δ + MDV) = 7.5. In this case, the contribution from the previous pulses in the signal did not exceed 10% of the maximum accumulated signal. The values of the maximum possible repetition-rate of system II is represented in the table below.

Here, the following notation was used: $l\tau_0$ – the pulse duration τ_0; l_Δ - the interval between pulses in meters; f – the frequency of pulses; M – the number of the accumulation cycles; E_o

$l\tau_0$ (km)	1	2	3	4	5	10	15	30
τ_0 (μs)	3,3	6,7	10,0	13,3	16,7	33.0	50,0	100,0
σ (km^{-1})				0,01 - 0,1				
lΔ (km)				30				
f (kHz)	9,7	9,4	9,1	8,8	8,6	7,5	6,7	5,0
M	581 000	562 000	546 000	528 000	516 000	450 000	400 000	300 000
E_0 (μJ)	51,6	53,4	54,9	56,8	58,1	66,7	74,6	100,0
W_0(W)	15,6	8,0	5,5	4,3	3,5	2,0	1,5	1,0
σ (km^{-1})				0,3				
lΔ (km)				11,7				
f (kHz)	23,6	21,9	20,4	19,1	17,9	1`3,9	11,2	10,4
M	1 420 000	1 310 000	1 220 000	1 150 000	1 080 000	830 000	670 000	620 000
E_0 (μJ)	21,0	23,0	24,0	26,0	28,0	36,0	45,0	48,0
W_0(W)	6,4	3,4	2,5	2,0	1,7	1,1	0,9	0,8
σ (km^{-1})				1.0				
lΔ (km)				3,5				
f (kHz)	66,7	54,5	46,1	40,0	35,3			
M	4 000 000	3 300 000	2 800 000	2 400 000	2 100 000	**fE_0 =const**		
E_0 (μJ)	7,5	9,2	10,8	12,5	14,2			
W0(W)	2,3	1,4	1,1	0,9	0,8			
σ (km^{-1})				10.0				
lΔ (km)				0,35		**W_0 = 0,5 W**		
f (kHz)	666,7	545,4	461,5	400,0	352,3			
M	40 000 000	33 000 000	28 000 000	24 000 000	21 000 000	**$E^{(2)}_{\Sigma} = E^{(1)}_{\Sigma}$**		
E_0 (μJ)	0,7	0,9	1,1	1,2	1,4			
W_0(W)	2,3	1,4	1,1	0,9	0,8			

Table 7. The maximum possible pulse repetition frequency (f) of the radiation remote-sensing systems (type II) depending upon the environment (σ).

– the energy of the radiation. This provides an accuracy that is not worse than the accuracy of the measurement system II for the same values of the extinction coefficient (σ). The number of emitted photons is equal in all the simulated cases. This corresponds to the radiation energy of system I for a full-time measurement (60 sec), which corresponds to the average power W_0 = 0.5 W. This allows us to visually compare systems with different types of organisation of the radiation source. Likewise, we assessed the limiting frequencies of the pulses of radiation systems for system III. The data obtained is summarised in the following table:

σ (km^{-1})	lτ_0	τ_0 (μs)	lΔ (m)	f (kHz)	M	E_0 (μJ)	W_0 (W)
0,01	30,0	100	60	10	600 000	50,0	0,5
0,1	30,0	100	60	10	600 000	50,0	0,5
0,3	16,7	55,7	60	18	1 100 000	28,0	0,5
1,0	5,0	16,7	60	60	3 600 000	8,4	0,5
10,0	0,5	1,7	60	600	36 000 000	0,9	0,5

Table 8. The maximum possible pulse repetition frequency of the radiation remote-sensing systems depending upon the environment (type III).

The necessary energy radiation does not exceed ten microjoules at the limiting frequencies. This suggests the use of low-power lasers as radiation sources in systems II and III, with optical shutters which open with a given frequency (f). The maximum frequency is obtained at ~ 1 MHz, but it has a range of 10-100 kHz in most cases. This is achieved by conventional optical shutters.

In the above conditions, the maximum pulse power of system II does not exceed 18W. For system III, the power is equal to 0.5W which is sufficient to achieve a measurement error not worse than tenths of a percent, excluding the errors caused by the instrument.

4.3 The simulation results of the signal structure stability of remote-sensing

We investigated the behaviour of three sample models in relation to the signal from a self-organising environment. The behaviour of the three sample models was analyzed. It has a 16-17 readout and a digitisation step - 30 minutes, with total duration of measurements from 12 to 17 days.

The averaging of the intervals between local maxima and minima gives the generalised intervals of the structure of the inhomogeneities (M+, M-).

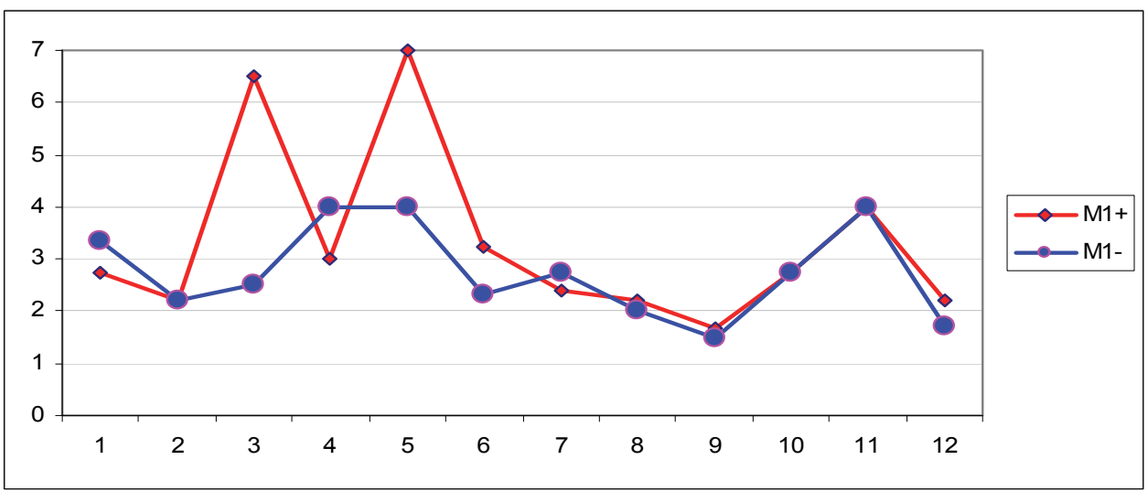

Fig. 7. Results of the interval definition between the elements of the generalised structure of different types, 'plus' and 'minus' (M+, M-) for some areas (1-12).

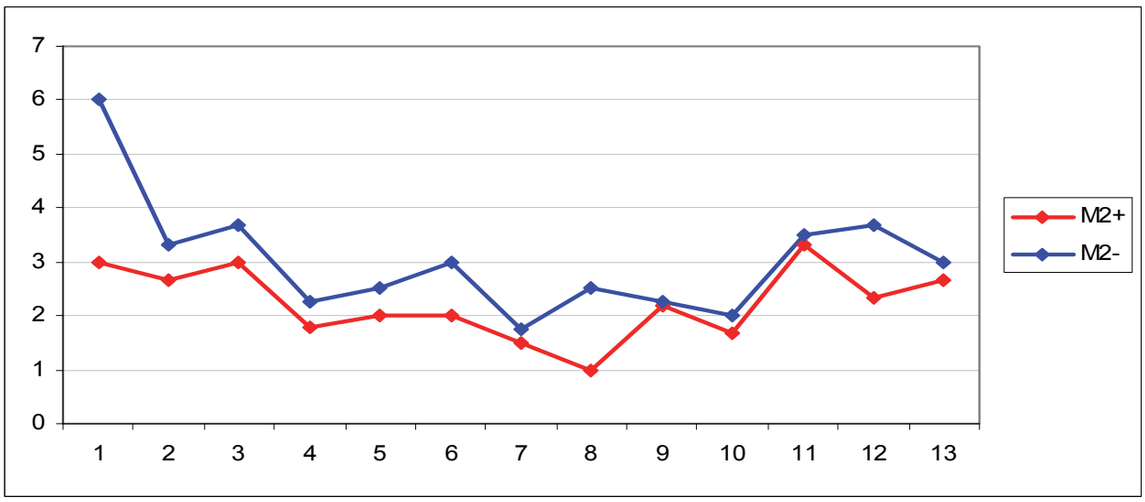

Fig. 8. Results of the interval definition between the elements of the generalised structure of different types, 'plus' and 'minus' (M+, M-) for some areas (1-13).

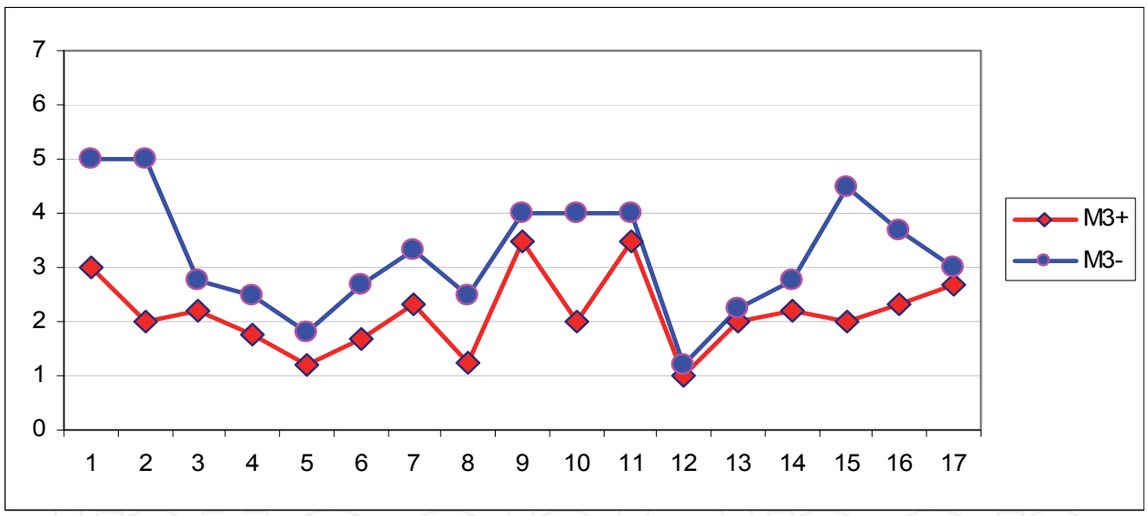

Fig. 9. Results of the interval definition between the elements of the generalised structure of different types, 'plus' and 'minus' (M+, M-) for some areas (1-17).

The interval size changes between the elements of the generalised structure as 'plus' or 'minus' has a complex character:

For the first sample, the peak growth of the interval sizes for the 'plus' structure (several times) in the third and fifth day is observed. It takes place against a wavy course of the 'minus' structure signal. The character of the change of the 'plus' and 'minus' structures actually coincides with each other in the range of the 9-12 day.

For the second sample, the waviness, falling down character of the dependence, with some subsequent general lifting and the constant prevalence (leadership) of the 'minus' signal structure, is characterised.

For the third sample, we see the integral character and the mutual position of the structures, which repeats the second sample at more of the pulse character of the ’minus‘ signal structure.

This is probably an estimation of the revealed structure of the corresponding dispersion (D+, D-).

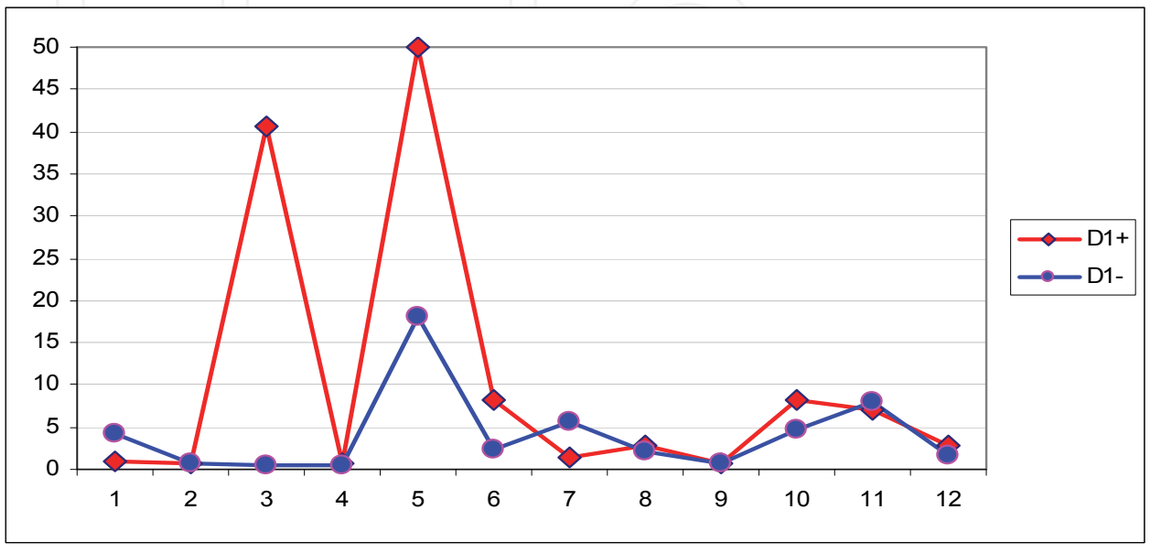

Fig. 10. The results of the dispersion definition between the elements of the generalised structure of different types, ’plus‘ and ’minus‘ (D+, D-) for some areas (1-12).

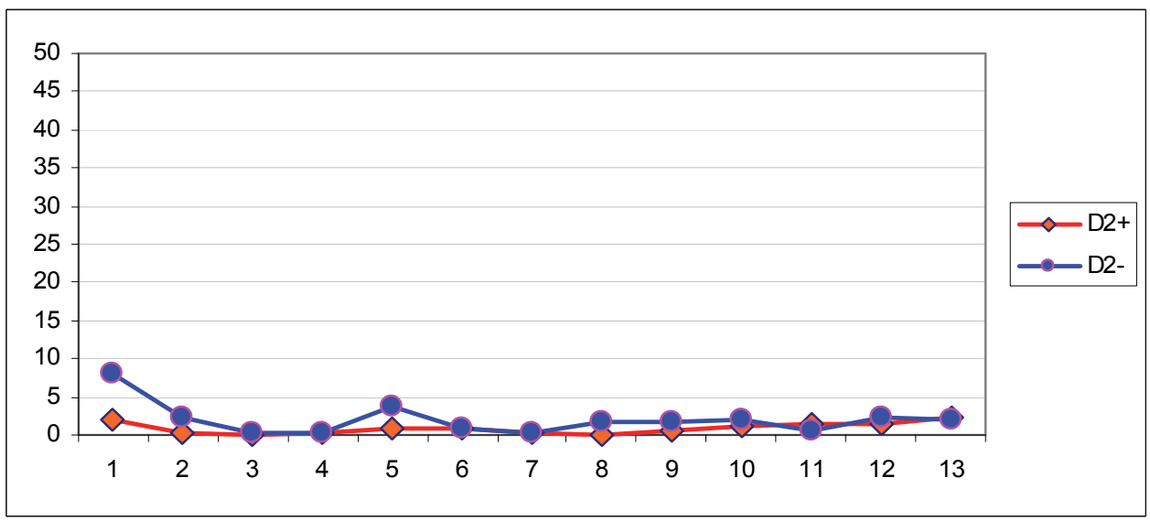

Fig. 11. Results of the dispersion definition between the elements of the generalised structure of different types, ’plus‘ and ’minus‘ (D+, D-) for some areas (1-13).

Change of the dispersion of an interval between the elements of the signal structure 'plus‘ and ’minus‘ has the following character:

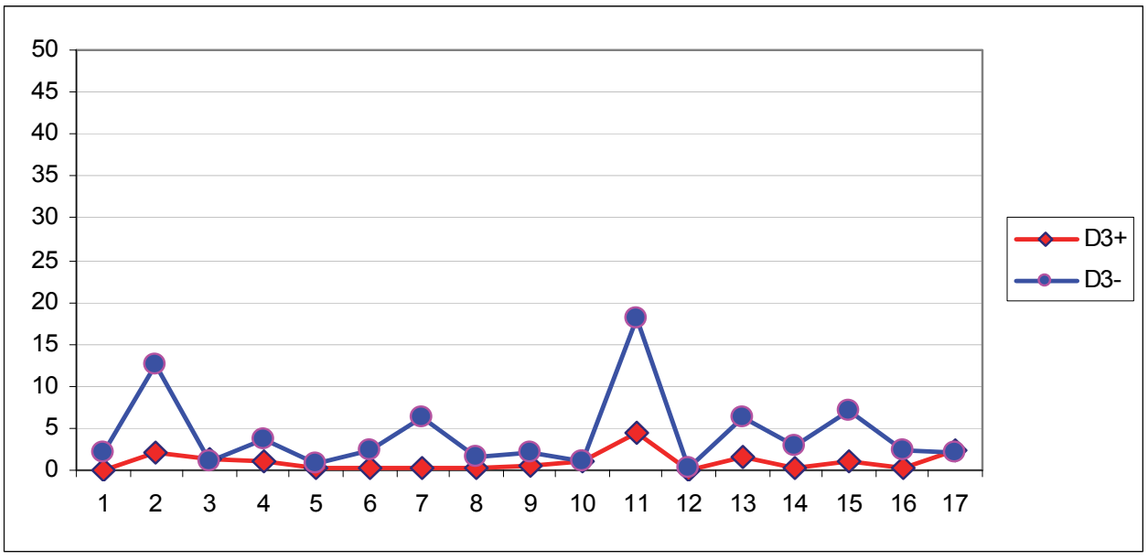

Fig. 12. Results of the dispersion definition between the elements of the generalised structure of the different types, 'plus' and 'minus' (D+, D-) for some areas (1-17).

For the first sample, the behaviour was similar to the behaviour of the intervals, i.e. the peak growth of the dispersion (instability) of the plus' structure intervals (several times) for the third and fifth day, and against a wavy course the 'minus' structure is characterised.

For the second sample, as well as for intervals, a poorly wavy character of dependence, with a constant prevalence (leadership) 'minus' structure is characterised.

For the third sample, the general character and mutual position of the structures has more pulse character, with emissions in the behaviour structure 'minus' for the second and eleventh day.

For a fuller analysis, additional characteristics have been used:

W – The regularity index; the average probability of the sample regular 'plus', 'minus' structure filling.

S – The connectivity index, the generalised difference of the probabilities of the sample regular 'plus', 'minus' structure filling.

The regularity index (W) of the frequency of the regular structure of the inhomogeneities shows that the probability of filling of the regular sample of the inhomogeneities at a certain interval (I = 1-13) is close to 0.5 only in the case where there is a sufficiently steady structure.

The characteristic tendency - the general course of curve W (I) is a little below the line 0,5. Essentially, the different behaviour of the regularity index (W) for the 'plus' and 'minus' structures is observed.

The W (I) of the 'minus' structure has a wavy character and actually does not reach the values 0,5. The W (I) of the 'plus' of the structure has a peaking characteristic and can reach values essentially more than 0,5 i.e. to fill all the sample.

It is probably necessary to draw a conclusion - the general excess of the level of probability 0,5 ‘plus’ to for “plus” structures with big emissions W (I) ’plus‘ against the smooth behaviour of W (I) ’minus‘ can be a criterion for the displacement of the general course of an analysed signal towards its lifting.

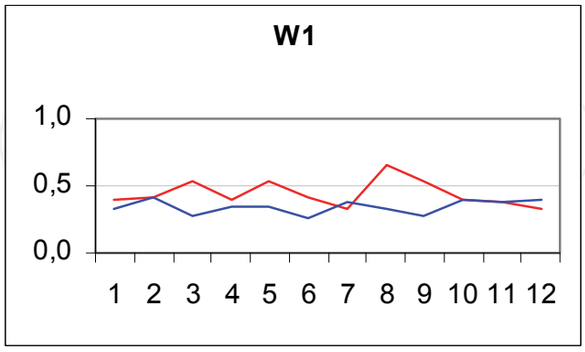

Fig. 13. The results of the calculation of the regularity index for the three situations presented above for the regular structure (W1).

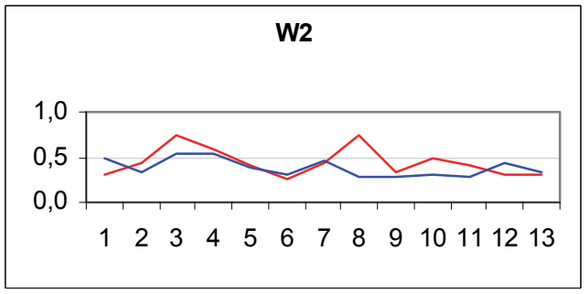

Fig. 14. The results of the calculation of the regularity index for the three situations presented above for the regular structure (W2).

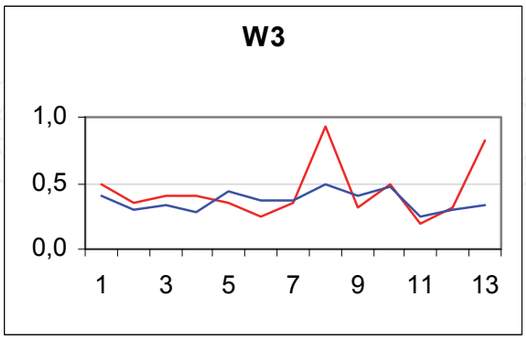

Fig. 15. The results of the calculation of the regularity index for the three situations presented above for the regular structure (W3).

The connectivity index (S) of the ’plus‘ and ’minus‘ structures is equal to zero and corresponds to a case of the behaviour synchronisation of the ’plus‘ and ’minus‘ structures, as a uniform structure of a harmonious type.

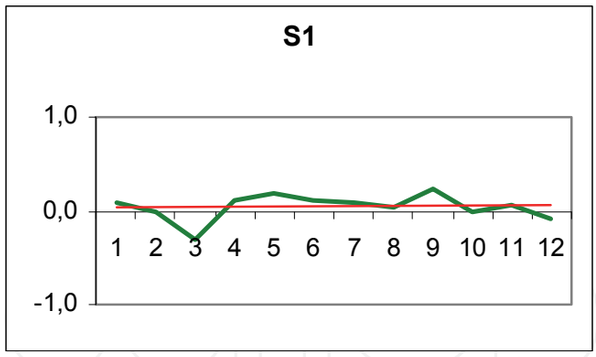

Fig. 16. The results of the calculation of the regularity index for the three situations presented above for the regular structure (W1).

The displacement of the connectivity index (S) in the ′plus′ and ′minus′ zone specifies on increase in the influence of ′plus′ and ′minus′ structures with an increase in the independence of their behaviour, rather than each other.

The displacement of the connectivity index (S) in a ′plus′ zone can be interpreted as the presence of the leader-structure of the ′plus′ type.

The displacement of an index of connectivity (S) in the ′minus′ zone can be interpreted as the presence of the leader- structure of the ′minus′ type.

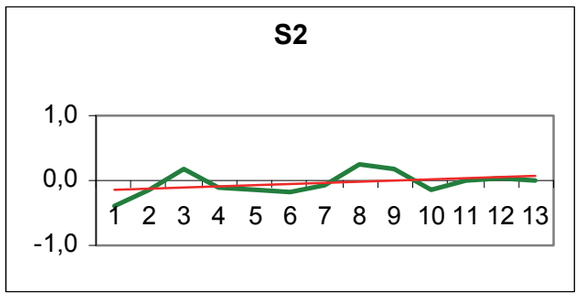

Fig. 17. The results of the calculation of the regularity index for the three situations presented above for the regular structure (W2).

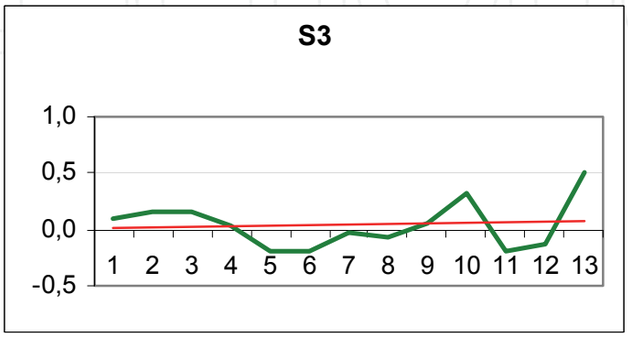

Fig. 18. The results of the calculation of the connectivity index for the three situations presented above for the regular structure (W3).

On the basis of the assumptions made, it is possible to draw the following conclusions:

For first sample, the connectivity index S1 (I) specifies the stable leader-structure of the 'plus' type.

For the second sample, the connectivity index S1 (I) specifies the transition of leadership from the structure of the 'minus' type to the structure of the 'plus' type.

For the third sample, the of connectivity index S3 (I) specifies the steady growth of the leadership of the structure of the 'plus' type.

The conclusion about the displacement of the general course of an analysed signal towards its general growth proves to be true in the presence of the 'plus' of leader-structures in all three samples of a signal, as the above results show.

5. Conclusion

5.1 Measurements

These estimates allow us to make some significant findings:

1. Increasing the accuracy of the measurement of the scattering signal can be achieved through the use of the described methods of the signal processing, long laser impulses or dark laser impulses.
2. This approach allows more accurate measurement of the scattering signal, by at least an order of magnitude, as well as measurements during the daytime up to distances comparable with the meteorological visibility range (MDV), including the area of multiple scattering.
3. The proposed system of remote measurement organisation allows us to solve existing contradictions and provides a specified signal/noise ratio under a wide range of conditions and at different times for remote tracks, and it allows the more accurate linking of the principles of recording equipment with the methodology of interpreting the data.
4. The application of the proposed approach to the principles of the construction of lidar systems allows us to use low-power light sources and, in a large measure, to get rid of hardware errors caused by shock loads on the receiving system.
5. This organisation of remote sensing systems allows us to pass from the problem of signal detection with high accuracy to the problem of minimising the distortion of the received signal, which is caused by instrumental factors.
6. The system with the probe interval (dark pulse) between impulses (type III) is the greatest prospect and it retains all of the advantages of systems of type II but with more performance.

The results obtained allow for a new approach to the problem of reconstructing the characteristics of the environment based upon remote sensing. It is not correctly solved for a real, heterogeneous environment, largely due to the exclusion of the consideration of thermodynamic processes (Polkanov, Y. A. et al., 1991).

5.2 Processing

1. "Leadership 'plus' structure" and "Leadership 'minus' structure" specifies, accordingly, the general lifting or falling of the signal.

2. "Leadership interception" specifies the tendency of change for the signal, from lifting to falling or the reverse.
3. Changing character of the structure means that the stability of the leadership of corresponding structure is subject to regular fluctuations ('plus' → 'minus' or 'minus' → 'plus').
4. The pointed character of the structure speaks about the obvious local tendency to change of the leadership of the corresponding structure.
5. The regularity of the revealed structure has an alternating character.
6. The higher the regularity, the higher the relative stability of the corresponding structure.
7. The higher the bond of the 'plus' and 'minus' structures, the higher their overall stability, even if intermittency has obvious characteristic.
8. The regular structure is the reason for the event both of a time interval corresponding to the taken measurements and that taken out of it, i.e. in the short-term and in the long-term plan.
9. The abnormal structure was the reason for the event, and not only in a time interval corresponding to the taken measurements, i.e. only in the short-term plan, as the regular structure smoothes out a special filtration.

For today's problems with remote sensing, it is necessary to apply the described methods of conflict resolution logic to the problem of reconstructing the characteristics of the environment. Then, the problem of measuring and processing the measurement results will be examined as a single complex. The extension of this logic leads to new tasks - the assessment of the impact of thermodynamic processes on the structure of inhomogeneities in the medium and their self-organisation and the development of criteria for the stability of such structures as indicators of self-protection and self-organisation (Polkanov, Y. A. et al., 200).

6. References

Ablavskij L.M. and Kruglov P.A. Main Geophysical Observatory Labour(in Russian), v.340, p.25, 1974

Ashkinadze D.A. and Belobrovik V.P. and Spiridovich A. L. and Kugeiko M.M. and Polknov Y.A. *Lidar determination of the dynamics of the fields of aerosol pollution in cities.* In the book.: VI Proc. Sympos. the laser and acoustic sensing. Proc. Part 1. Tomsk, 1980. 152-155.

Kovalev V.A. Main Geophysical Observatory Labour (in Russian), v.312, p.128, 1973

Mingming Feng, Kevin L. Silverman, Richard P. Mirin, and Steven T. Cundiff. *Dark pulse quantum dot diode laser.* Optics Express, Vol. 18, Issue 13, pp. 13385-13395, 2010 doi:10.1364/OE.18.013385
http://www.opticsinfobase.org/abstract.cfm?URI=oe-18-13-13385

Polkanov Y.A. *The opportunities of a mode of the photon account at registration of the dispersion signal of laser radiation in an atmosphere.* Radiotechnika i Electronuka (Radio engineering and electronics), 1983, v. XXVIII, № 10, p. 2080-2082. http://adsabs.harvard.edu/abs/1989Prib...32....6P

Polkanov Y.A. *On regular structure of scattering inhomogeneities for optical radiation in the atmosphere.* Izvestia Akademii Nayk SSSR. Seriya Rhizika Atmospheryi I Okeana

(News of the Academy of sciences of the USSR. Physics of an atmosphere and ocean), 1985 v. 21, № 7, p. 720-725.

Polkanov Y.A. and Ashkinadze D.A. *The opportunities of increase of the signal accuracy of optical radiation dispersion in an atmosphere*. Radiotechnika i Electronuka (Radio engineering and Electronics). 1988, v. 12, p. 2599-2603.
http://adsabs.harvard.edu/abs/1988RaEl...33.2599P

Polkanov Y.A. and Kudinov V. N. *A possibility for the analysis of the periodic structure of a complex signal*. Priborostroenie. 1989. V.32. № 4. P.6-11.
http://adsabs.harvard.edu/abs/1989Prib...32....6P

Polkanov Y.A. *One opportunity of the periodic structure analysis of a complex signal.* Izvestia Vysshich Uchebnych Zavedenij, Priborostroenie (News of high schools. Instrument making). 1989, v. 32, № 4, p. 6-11.

Polkanov Y.A. The *dynamic structure of a scattering signal and its connection with meteorological situation*. Izvestia Akademii Nayk SSSR. Seriya Optika Atmospheryi I Okeana (News of the Academy of sciences of the USSR. Physics of an atmosphere and ocean), 1989 v. 25, № 6, p. 599-603.

Polkanov Y.A. *Matchig between a change in the structure of atmospheric optical inhomogeneities and a set of meteorological parameters.* Meteorologiya I Gidrologiya (Meteorology and hydrology) 1991, № 3, p. 39-48.
http://cat.inist.fr/?aModele=afficheN&cpsidt=5237241

Polkanov Y.A. *A possibility of detecting anomalous inhomogeneties of the atmosphere (the Method of a nonlinear filtration of the return dispersion signal)* Izvestia Akademii Nayk SSSR. Seriya Optika Atmospheryi I Okeana (News of the Academy of sciences of the USSR. Physics of an atmosphere and ocean), 1992 v. 5, № 7, p. 720-725.
http://pdf.aiaa.org/jaPreview/AIAAJ/1994/PVJAPRE48291.pdf (Publication Date: 04/1994)

Polkanov Y.A. *Accuracy of the representation of the real scattering signal in terms of the lidar equation.* Journal of Applied Spectroscopy. Springer New York. 0021-9037 (Print) 1573-8647 (Online). Volume 37, Number 3 / September, 1982. p. 1091-1095. SpringerLink Date Tuesday, December 07, 2004.
http://www.springerlink.com/content/g532t57564377366/

Polkanov Y.A. *Sounding of the environment by means of the un-impulse of the low-power continuous source*. Proceedings of SPIE -- Volume 6750 Lidar Technologies, Techniques, and Measurements for Atmospheric Remote Sensing III, Upendra N. Singh, Gelsomina Pappalardo, Editors, 67501H (Oct. 3, 2007) (published online Oct. 3, 2007)
http://spiedl.aip.org/getabs/servlet/GetabsServlet?prog=normal&id=PSISDG006750000001675 01H000001&idtype=cvips&gifs=yes

Polkanov Y.A. *Medium sensing by low-power strobe pulse.* Proceedings of SPIE -- Volume 6936 Fourteenth International Symposium on Atmospheric and Ocean Optics/Atmospheric Physics, Gennadii G. Matvienko, Victor A. Banakh, Editors, 693613 (Feb. 14, 2008) (published online Feb. 14, 2008)
http://spiedl.aip.org/getabs/servlet/GetabsServlet?prog=normal&id=PSISDG006936000001693613000001&idtype=cvips&gifs=yes

Polkanov Y.A. *Lidar measurements for the short-term forecast of meteorological stability* (Proceedings Paper) http://spie.org/x648.html?product_id=783368 (Publication Date: 02/2008)

Polkanov Y.A. *The structurally-statistical remote analysis of the self-organizing processes*.[7479-25] p. 31 Lidar Technologies, Techniques, and Measurements for Atmospheric Remote Sensing V Conference 7479 - Proceedings of SPIE Volume 7479Dates: Monday-Tuesday 31 August - 1 September 2009
http://www.google.com/search?client=opera&rls=ru&q=spie+2009+Polkanov+1.+The+structurally-statistical+remote+analysis+of+the+self-organizing+processes+in+an+complex+systems,+Yury+Polkanov&sourceid=opera&ie=utf-8&oe=utf-8

V. E. Zuev and M. V. Kabanov, *Transfer of Optical Signals in the Earth's Atmosphere* (in Russian), Sovetskoe Radio, Mosow 1977

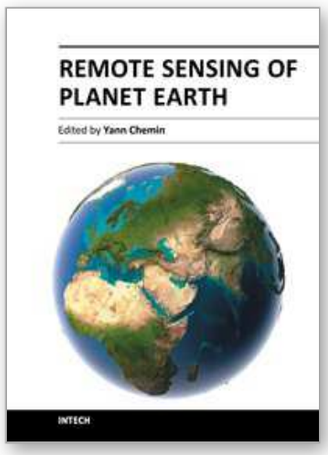

Remote Sensing of Planet Earth

Edited by Dr Yann Chemin

ISBN 978-953-307-919-6
Hard cover, 240 pages
Publisher InTech
Published online 27, January, 2012
Published in print edition January, 2012

Monitoring of water and land objects enters a revolutionary age with the rise of ubiquitous remote sensing and public access. Earth monitoring satellites permit detailed, descriptive, quantitative, holistic, standardized, global evaluation of the state of the Earth skin in a manner that our actual Earthen civilization has never been able to before. The water monitoring topics covered in this book include the remote sensing of open water bodies, wetlands and small lakes, snow depth and underwater seagrass, along with a variety of remote sensing techniques, platforms, and sensors. The Earth monitoring topics include geomorphology, land cover in arid climate, and disaster assessment after a tsunami. Finally, advanced topics of remote sensing covers atmosphere analysis with GNSS signals, earthquake visual monitoring, and fundamental analyses of laser reflectometry in the atmosphere medium.

InTech Europe
University Campus STeP Ri
Slavka Krautzeka 83/A
51000 Rijeka, Croatia
Phone: +385 (51) 770 447
Fax: +385 (51) 686 166
www.intechopen.com

InTech China
Unit 405, Office Block, Hotel Equatorial Shanghai
No.65, Yan An Road (West), Shanghai, 200040, China
中国上海市延安西路65号上海国际贵都大饭店办公楼405单元
Phone: +86-21-62489820
Fax: +86-21-62489821

IntechOpen